

# Numerical Modeling and Visualization of Supersonic Tip Vortices

T.V. Konstantinovskaya<sup>1</sup>, V.E. Borisov<sup>2</sup>, A.E. Lutsky<sup>3</sup>

Keldysh Institute of Applied Mathematics RAS

<sup>1</sup> ORCID: 0000-0002-1127-503X, [konstantinovskaya.t.v@gmail.com](mailto:konstantinovskaya.t.v@gmail.com)

<sup>2</sup> ORCID: 0000-0003-4448-7474, [narelen@gmail.com](mailto:narelen@gmail.com)

<sup>3</sup> ORCID: 0000-0002-4442-0571, [allutsky@yandex.ru](mailto:allutsky@yandex.ru)

## **Abstract**

Scientific visualization has taken a strong place among data analysis tools. Indeed, after all, its methods help not only to visualize the flow, but also to distinguish its main structures, to compare them, etc. The paper present application of visualization methods to analysis and comparison of a streamwise supersonic tip vortex pair interaction at the Mach number of the incoming flow  $M_\infty = 3$ . Maximum vorticity and the  $\lambda_2$  criterion were used for this purpose. A pair of supersonic vortices was generated by two coaxial straight wings with sharp front, side and trailing edges. Two configurations are considered: a pair of counter-rotational vortices and a pair of co rotational vortices. In the first case, the attack angle of the wings was  $+10^\circ$ , in the second - the attack angle of one wing was  $+10^\circ$ , of the second -  $10^\circ$ . Numerical data were obtained in the region of 10 wing chords downstream from the wing axis using a numerical model based on URANS equations with the turbulence model SA. Numerical simulations were carried out on the K-60 hybrid supercomputer system at the Keldysh Institute of Applied Mathematics of the Russian Academy of Sciences using the developed ARES software package for modeling 3D turbulent flows on high-performance computer systems. The main simulations were performed using 224 processors. Simulations were carried out on unstructured grids with hexagonal cells. The paper also shows an example when commonly used visualization methods application leads to some ambiguousness, because they give false additional vortex zones.

**Keywords:** supersonic flow, vortex identification, supersonic tip vortex, vortex pair, scientific visualization tools.

## **Introduction**

In the modern world with widely and actively developing technologies, there is a high interest in the development of supersonic aircraft both in the military and in the civil aviation. In particular, an important task of aerodynamics is to study a pair of tip vortices, since various vortex structures are formed during the flight of any aircraft on the edges of various aircraft elements, including wings. The vortex wake hazard of any aircraft for the following aircraft is well known [1]. Furthermore, a vortex wake risk to get on other downstream elements of the aircraft especially in the supersonic modes. It can also get fall into combustion chamber of propulsion system [2]. All of the above can affect the movement and control of the aircraft up to the complete loss of its control. Subsonic tip vortices have been studied quite well, while supersonic vortices need further study under various regimes.

Special visualization methods of vortex flows, in particular, are used for post-processing, analysis and comparison of the obtained data. The corresponding extensive reviews were made, for example, in [3-7].

In this paper the comparing results of supersonic tip vortex pair propagation by the scientific visualization methods are presented. Two pair configurations were considered:

counter-rotating and co-rotating. The method of maximum vorticity and the  $\lambda_2$  criterion for visualization of vortex structures were used in the process of analysis and comparison.

The authors are engaged in a comprehensive study of the particular problem - the problem of propagation, development and interaction of supersonic tip vortices. Scientific visualization methods are one of the tools used by the authors in their work, and not the subject of study. For the first time, the authors used the methods of scientific visualization in [8]. Thus, the authors do not aim to compare and study the methods of scientific visualization, but only apply them in their research.

Of course, scientific visualization is an important stage of data research, allowing for their analysis. However, do not forget about the limitations associated with the use of scientific visualization methods. Below we will give an example of data, when the application of the already mentioned  $\lambda_2$  method, as well as the  $Q$  method leads to the appearance of an "artifact" vortex and gives a false picture of the flow.

## Problem Statement

Visualization methods were used to perform a comparative analysis of data obtained by numerical modeling of a counter- and co-rotating supersonic vortex pair at the Mach number of the incoming flow  $M_\infty = 3$ . The attack angles of the wing-generators to the incoming flow for the case of counter rotation were  $10^\circ$ , and for the case of co-rotation, the attack angle of the one wing was  $10^\circ$ , and of the other was  $-10^\circ$ .

The flow behind two coaxial wings with sharp leading, trailing, and side edges and with a diamond-shaped base was numerically investigated and compared (fig.1). The wings were attached by the base to the walls which are parallel to the flow direction. The model configuration of the case of a counter-rotating pair completely coincides with the one described in [9]. The model configuration for the case of a co-rotating pair differs by rotating one of the generator wings to the position  $-10^\circ$  to the incoming flow (wing 1 was rotated, fig.1).

A unit of length was taken  $L = 1$  m. Density and pressure were non-dimensionalized by its free stream values [10]. The dimensions of the numerical domain were as follows:  $L_x = 0.35$ ,  $L_y = 0.225$  and  $L_z = 0.2$ . The geometry of the used wings was the same for the both configurations considered: the chord of each wing was equal to  $b = 0.03$ , half-span of the first wing was  $l_1 = 0.075$ , of the second one was  $l_2 = 0.095$ . The thickness of the diamond-shaped base of the both wings was equal to  $h = 0.004$ . The distance between the tip chords of the wings was  $l_3 = 0.03$ . So the width of the area between the walls was  $H = 0.2$ . The  $x$  axis was co-directed to the incoming flow. The  $z$  axis coincided with the common axis of the wings. The  $y$  axis was directed from the leeward side of the wings to the windward side (it implies the sides of the counter-rotation case or of the second wing, the rotation of which remains unchanged for both considered cases). The length of the numerical domain under consideration was up to 10 wing chords downstream from the common axis of the wings. The Reynolds number in simulation was  $Re_L = 1 \times 10^7$ .

## Numerical Simulation

Numerical modeling was carried out on the supercomputer K-60 at the Keldysh Institute of Applied Mathematics of the Russian Academy of Sciences [11] using the software package ARES developed by the authors [12] for calculating three-dimensional turbulent flows of viscous compressible gas on high-performance computing systems. The numerical method is based on the solution of unsteady Reynolds averaged Navier-Stokes equations (URANS) with the Spalart-Allmaras turbulence model [13, 14]. The finite volume method was used with reconstructions of the 2nd (TVD) and of the 3rd (WENO) orders for space discretization of the equations. The temporal approximation was performed on the basis of an explicit scheme. The numerical algorithms are described in more details in [15]. An unstructured hexagonal mesh was used for simulations. The mesh consisted of 25,774,200 cells for the case of a

counter-rotating vortex pair and of 35,763,750 for a co-rotating pair. The mesh was fined in the zone of vortices formation and propagation for better resolution of vortex structures. The difference in the number of cells is due to the mesh rearrangement and to the fact that in the first considered case mesh refinement was carried out on one side of the wings, and in the second – on both sides according to the location of the tip vortices. Simulations were carried out on 224 processors.

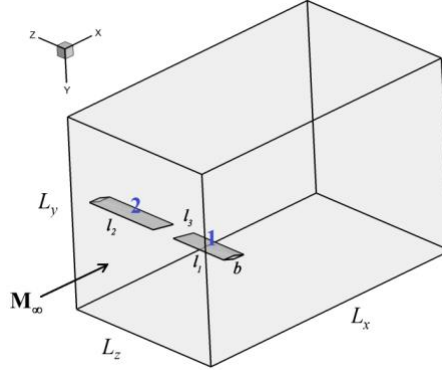


**Figure 1.** General model scheme: counter-rotating case

## Vortex Visualization

A separate post-processing data simulation module was developed for determining, in particular, vortex structures for hexagonal grids within the developed software package. Same scientific visualization methods were fully implemented in it. Among them, the maximum vorticity method and the  $\lambda_2$  method are realized. The module generates data of vortex structures in the format of the Tecplot software package, which is used for further visualization of numerical simulation results.

Despite the fact that there is still no unambiguous definition of a vortex [7, 16, 17], the definition of a vortex as the rotational motion of matter particles around the center is intuitively clear. The measure of this movement is the vorticity. The vorticity of the flow is defined as the vector product  $\boldsymbol{\omega} = \nabla \times \mathbf{u}$  that is the curl of velocity  $\mathbf{u}$ .

The velocity gradient tensor  $\nabla \mathbf{u}$  can be decomposed into symmetric and antisymmetric parts like

$$\nabla \mathbf{u} = \mathbf{S} + \boldsymbol{\Omega}, \quad S_{i,j} = \frac{1}{2} \left( \frac{\partial u_i}{\partial x_j} + \frac{\partial u_j}{\partial x_i} \right), \quad \Omega_{i,j} = \frac{1}{2} \left( \frac{\partial u_i}{\partial x_j} - \frac{\partial u_j}{\partial x_i} \right),$$

where  $\mathbf{S}$  and  $\boldsymbol{\Omega}$  are the strain-rate and vorticity tensors of the flow respectively.

### $\lambda_2$ -method

The  $\lambda_2$ -method (or criterion) of vortex identification was proposed in [18]. According to this criterion, the vortex flow region is determined based on the analysis of the eigenvalues of the always real symmetric matrix  $\mathbf{A} = \mathbf{S}^2 + \boldsymbol{\Omega}^2$ .

According to this method the vortex region is considered to be the part of space in which the second eigenvalue  $\lambda_2(\mathbf{A}) < 0$  ( $\lambda_1 \geq \lambda_2 \geq \lambda_3$ ). This method is quite widespread and is often used in data processing. Under adiabatic conditions, this criterion guarantees an instantaneous pressure minimum in a two-dimensional flow [16].

### Maximum vorticity method

The maximum vorticity method was proposed in [19]. It is based on one of the definitions of vortex flow and consists in detection the local maximum of the vorticity vector modulus  $|\boldsymbol{\omega}| = |\nabla \times \mathbf{u}|$  in the plane which is perpendicular to the direction of this vector. This method allows to determine the exact axis of the streamwise vortex in the case of sufficient resolution of the computational mesh.

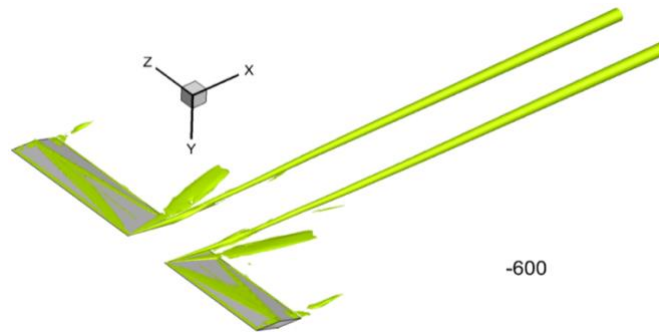
## Visualization methods application results

In this part of the paper the results of the analysis and comparison of the mentioned numerical data by visualization methods are presented.

### Counter-rotating supersonic vortex pair

The application of the  $\lambda_2$  and of the maximum vorticity visualization methods of vortex structures to the considered configuration of counter-rotating supersonic vortex pair was demonstrated in [9]. Let's repeat the main results here.

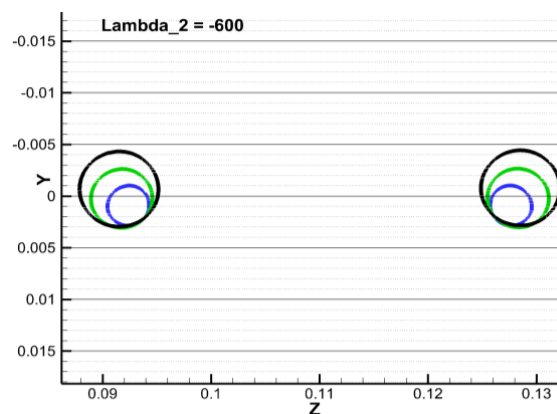
The  $\lambda_2$ -method makes it possible to determine a zone of the vortex flow. In our case it is the vortex cores. The results of its application to the counter-rotating supersonic vortex pair are shown on fig. 2, on which the isosurfaces of  $\lambda_2 = -600$  are visualized.



**Figure 2.** The application result of the  $\lambda_2$  visualization method to a pair of counter-rotating supersonic tip vortices, isosurface of level  $\lambda_2 = -600$  (yellow-green)

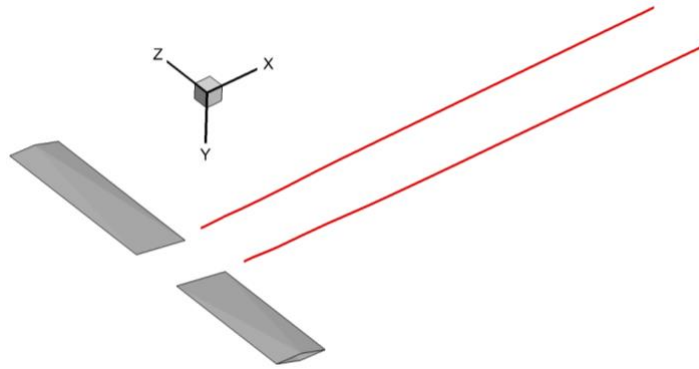
Figure 3 shows the lines of the level  $\lambda_2 = -600$  in sections that are perpendicular to the incoming flow direction:  $x = 0.1$  (blue circle),  $x = 0.2$  (green circle),  $x = 0.3$  (black circle). There is an increase in the diameter of the vortex core as it moves downstream from the wing-generators axis.

The displacement of counter-rotating supersonic vortices to leeward is noted, which correlates with the data of other authors [20] and with dynamics of line vortices in two-dimensional incompressible flow [21], and their repulsion from each other downstream from the wing axis at the considered distance is also noted.



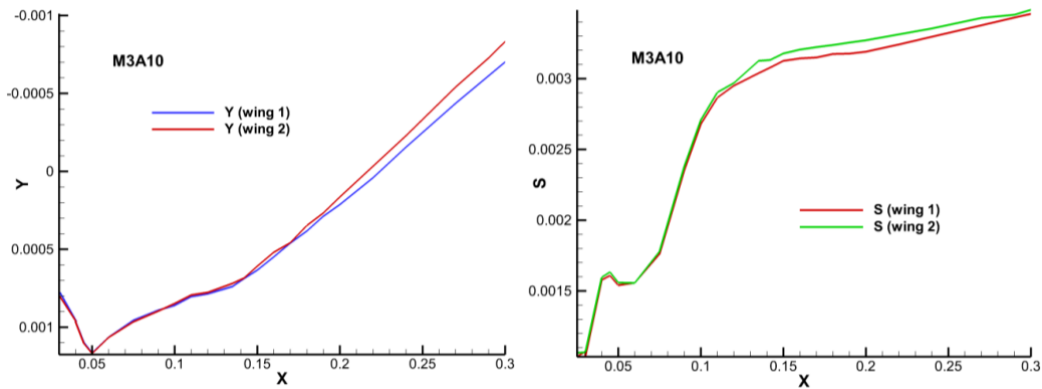
**Figure 3.** Lines of level  $\lambda_2 = -600$  in cross-sections  $x = 0.1$  (blue line),  $x = 0.2$  (green line),  $x = 0.3$  (black line), counter-rotating vortices

The application result of the maximum vorticity method to the counter-rotating supersonic vortex pair is shown on figure 4, it defines the axes of the vortices.



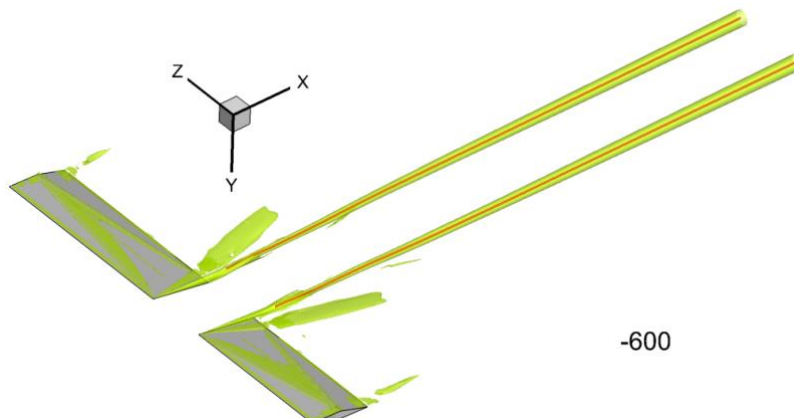
**Figure 4.** Axes of counter-rotating supersonic vortex pair determined by the maximum vorticity method (red lines)

Figure 5 shows plots of the vertical coordinate  $y$  of the axes and the variable  $S$  (the distance between the coordinate  $z$  of the vortex axis and the tip chord of the corresponding generator wing) for the counter-rotating vortex pair. These plots, as well as fig. 3, demonstrate the displacement of the axes of the vortices.



**Figure 5.** Axis coordinates of counter-rotating vortices:  $y$  (left) and  $S$  (right).

Figure 6 shows the results of the scientific visualization methods superposition: of the maximum vorticity and of the  $\lambda_2$ -criterion that were applied to the counter-rotating supersonic vortex pair: the red lines of the vortex axis are located inside the yellow-green vortex core (isosurface  $\lambda_2 = -600$ ). Both methods show correlated results and complement each other.

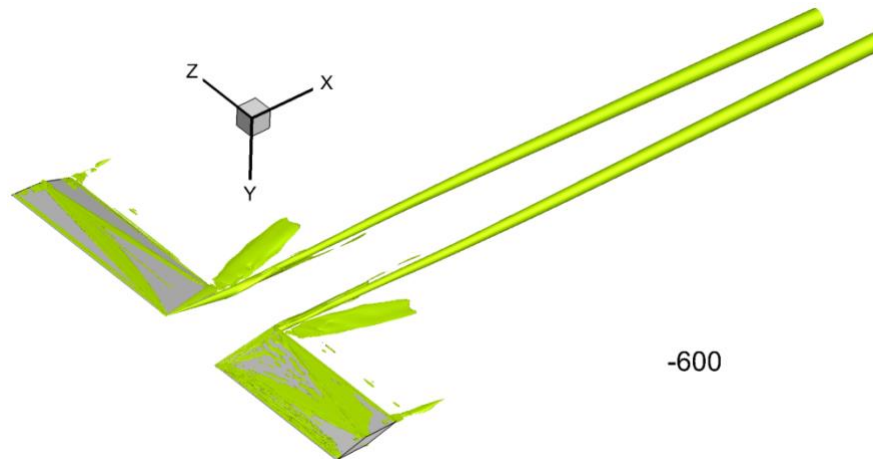


**Figure 6.** The superposition result of the axes of the counter-rotating vortex pair (red lines) found by the maximum vorticity method and of the vortex core obtained by the  $\lambda_2$  method, isosurface of level  $\lambda_2 = -600$  (yellow-green)

## Co-rotating supersonic vortex pair

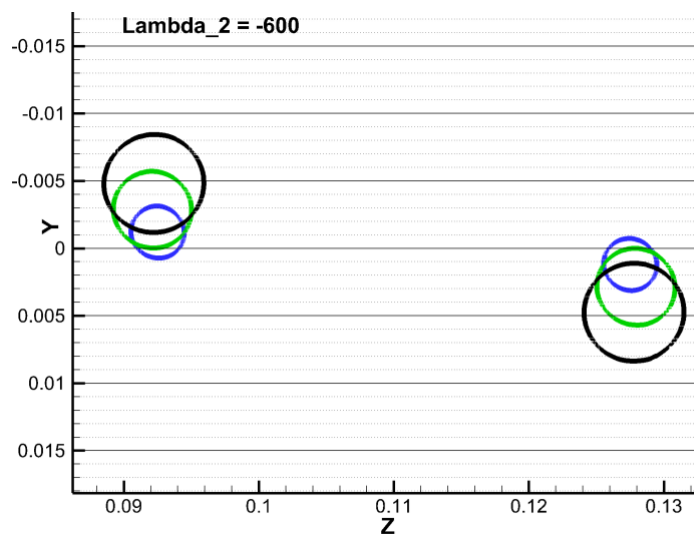
Further, the applying results of two mentioned visualization methods to a co-rotating supersonic vortex pair present in the paper.

Figure 7 shows the region of vortex propagation determined by the  $\lambda_2$  visualization method where the isosurfaces of  $\lambda_2 = -600$  are displayed.



**Figure 7.** The applying result of the  $\lambda_2$  visualization method to a pair of co-rotating supersonic tip vortices, isosurface of level  $\lambda_2 = -600$  (yellow-green)

Figure 8 shows the lines of the level  $\lambda_2 = -600$  in cross sections  $x = 0.1$  (blue line),  $x = 0.2$  (green line),  $x = 0.3$  (black line) which are perpendicular to the main flow direction. The diameter of the vortex cores increases downstream from the generator wings.



**Figure 8.** Lines of level  $\lambda_2 = -600$  in cross-sections  $x = 0.1$  (blue line),  $x = 0.2$  (green line),  $x = 0.3$  (black line), co-rotating vortices

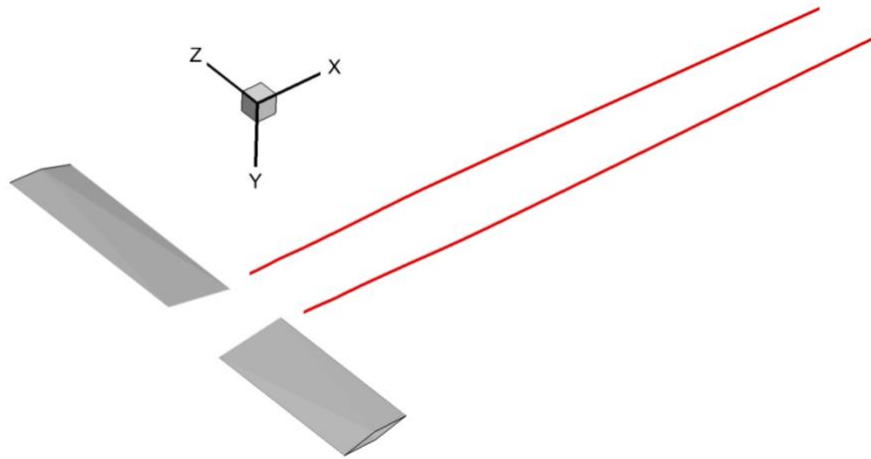


**Figure 9.** Axes of co-rotating supersonic vortex pair determined by the maximum vorticity method (red lines)

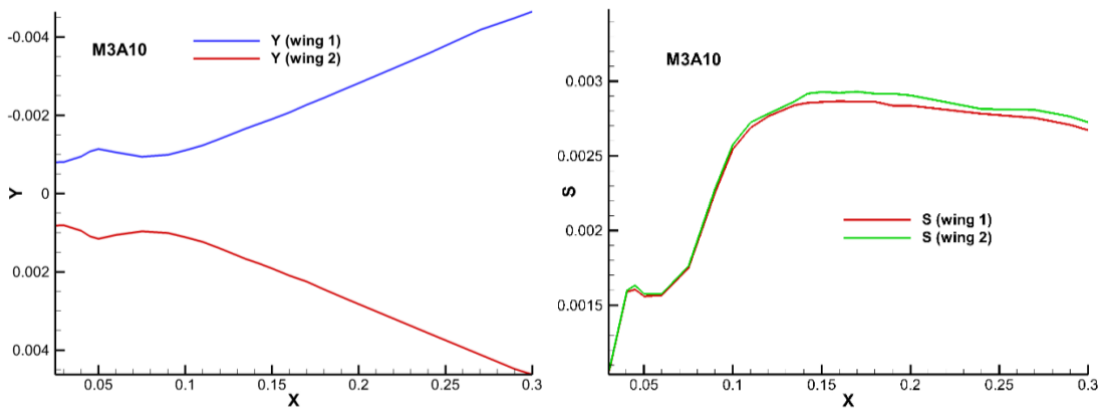
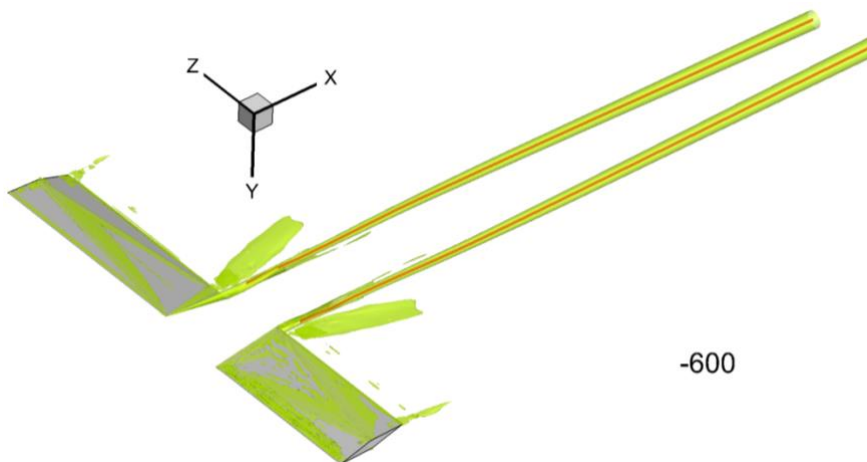


**Figure 10.** Axis coordinates of co-rotating vortices:  $y$  (left) and  $S$  (right).

The result of determining of the co-rotating supersonic vortex pair axes obtained by the maximum vorticity visualization method of vortex structures is shown in fig. 9.

Figure 10 shows plots of the displacement of the axes of the co-rotating supersonic vortex pair. It shows the change of the vertical coordinate  $y$  and of the variable  $S$  (the distance between the  $z$  coordinate of the vortex axis and the tip chord of the corresponding generator wing).



-600

**Figure 11.** The superposition result of the axes of the co-rotating vortex pair (red lines) found by the maximum vorticity method and of the vortex core obtained by the  $\lambda_2$  method, isosurface of level  $\lambda_2 = -600$  (yellow-green)

Thus the circular displacement of co-rotating supersonic vortices in the direction that coincides with the direction of vortices rotation is noted (fig. 8, 10). This correlates with the data of other authors [22] and with the dynamics of line vortices in two-dimensional incompressible flow [21]. Their simultaneous divergence from each other is also noted.

Figure 11 shows the joint position of the axes of the co-rotating supersonic vortex pair determined by the maximum vorticity visualization method (red lines) and of the vortex cores determined by the  $\lambda_2$  criterion (yellow-green isosurfaces  $\lambda_2 = -600$ ). The application results of both scientific visualization methods are in good agreement with each other.

### Example of erroneous definition of vortex structures

Since our working group is engaged in various studies in the field of supersonic vortices propagation and interaction, one day we came across a problem where the visualization methods we used earlier, namely the  $\lambda_2$  method, gives false vortex zones: it gives the presence of an artifact second vortex.

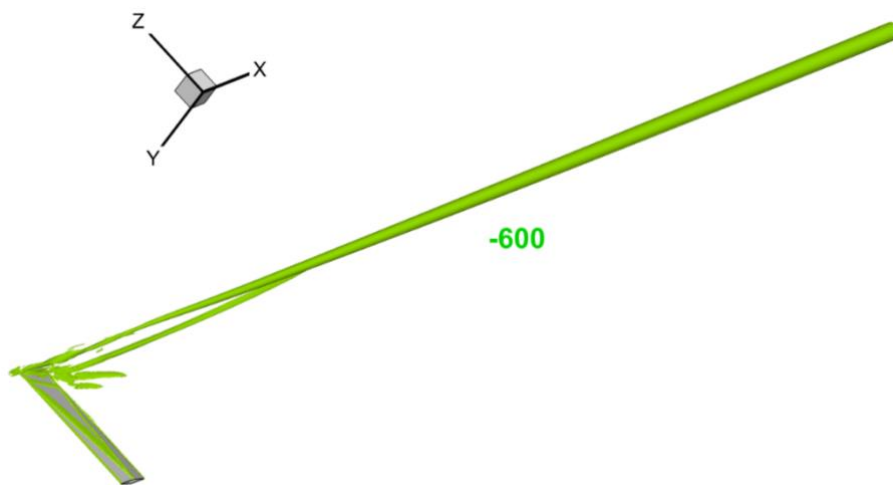


**Figure 12.** The applying result of the  $\lambda_2$  method to the problem of energy input upstream from the wing generator, isosurface of level  $\lambda_2 = -600$

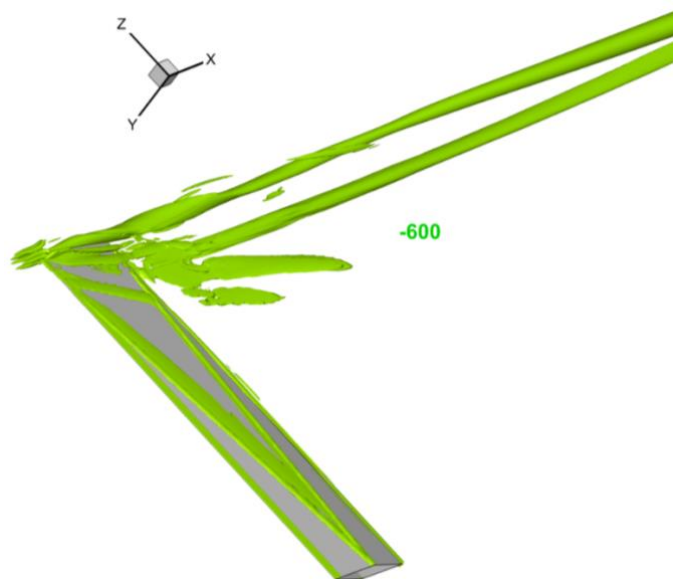


**Figure 13.** The applying result of the  $\lambda_2$  method to the problem of energy input upstream from the wing generator, isosurface of level  $\lambda_2 = -600$ , zoom on near distance

We are talking about the problem of energy input upstream from the wing generator. The applying result of the  $\lambda_2$  method to this problem is shown on the next figures (fig. 12, 13).



Obviously, there is a visible appearance of a second vortex, which then merges with the main one.

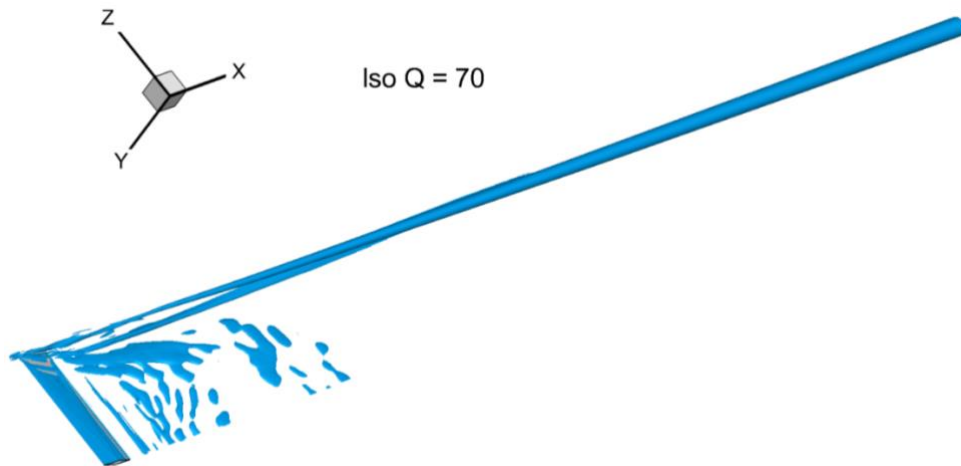


**Figure 14.** The applying result of the  $Q$  method to the problem of energy input upstream from the wing generator, isosurface of level  $Q = 70$

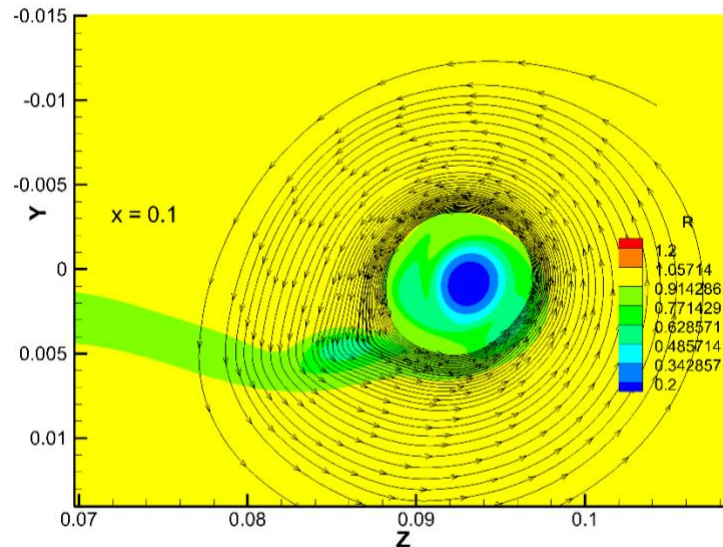


**Figure 15.** Density distribution and streamtraces in cross-section  $x = 0.1$

The application of the  $Q$  scientific visualization method (described in [23]) gives a similar result (see fig. 14). This method, as well as the  $\lambda_2$  method, is expressed in terms of matrices  $\mathbf{S}$  (strain-rate) and  $\mathbf{\Omega}$  (vorticity tensors) and under the assumption of incompressible flow is:

$$Q = \frac{1}{2}(\|\mathbf{\Omega}\|^2 + \|\mathbf{S}\|^2)$$

that is a measure of the local rotation rate in excess of the strain rate. Hence, a vortex region is defined at  $Q > 0$ .

However, additional studies show that there is no second vortex. This can be seen on the example of figure 15, which shows the density and streamtraces in a cross section  $x = 0.1$  located approximately in the middle of the "false double vortex" zone.

The authors do not aim to thoroughly investigate and describe the mentioned above task in this work, as well as to describe all scientific visualization methods, and only aim to show the case of the inapplicability of the mentioned visualization methods.

However, not so long ago, a new visualization method of vortex structures called Rortex appeared [24]. Later it was renamed Liutex in honor of one of the authors [25]. This method, unlike the others, excludes shift terms and takes into account only rotational ones. Its

application to the mentioned problem of an energy source in front of a wing generator will be the subject of our further research.

## Conclusion

The results of the analysis and comparison of a supersonic vortex pair interaction by scientific visualization methods at the Mach number of the incoming flow  $M = 3$  are reflected in the paper. Two methods were used: the  $\lambda_2$  criterion and the maximum vorticity method. Two configurations are considered: pairs of counter- and co-rotating vortices.

For numerical simulations of the analyzed data, the developed software package ARES for simulating three-dimensional turbulent flows was used. Simulations were carried out on 224 processors on the hybrid supercomputer system K-60 at the Keldysh Institute of Applied Mathematics of the Russian Academy of Sciences.

It is found that in both cases the vortices are longitudinal cone-shaped structures whose diameter gradually expands as they move downstream from the axis of the generator wings.

The axes of vortices are determined by the scientific visualization method of maximum vorticity. After the nonmonotonous zone associated with the vortex formation zone, the displacement of the vortices for both considered cases at the considered distances is shown. For the case of counter-rotating vortices, their displacement to the leeward side of the generator wings and their slight divergence from each other is observed. For the case of co-rotating vortices, the rotation of the vortices around each other in the direction coinciding with the direction of rotation in the vortex core is observed. Thus, there is a mutual influence of vortices on each other during their joint propagation.

These methods of scientific visualization perform well in many tasks. However, do not forget about the limitations associated with their use. So, in the course of our research, we got a case when the above methods do not work, i.e. they give an artefact vortex zone. Nevertheless, one of the latest visualization methods (Rortex or Liutex) seems promising and its application will definitely become one of the topics of our further research.

## References

1. Wake Turbulence Training Aid (section 2), FAA Report, DOT/FAA/RD-95/6 DOT-VNTSC-FAA-95-4, United States Department of Transportation, 1995.
2. Vergine F., Maddalena L. Study of two supersonic streamwise vortex interactions in a Mach 2.5 flow: Merging and no merging configurations. *Physics of Fluids*, **27**, 076102, 2015.
3. Hansen C.D., Johnson C.R. (Eds.). *The Visualization Handbook*. NY: Academic Press, 2004, 984 p.
4. Chakraborty, P., Balachandar, S., Adrian, R. G. On the relationships between local vortex identification schemes. *J. Fluid Mech.*, **535**, pp 189-214, 2005.
5. Kolář V. Brief Notes on Vortex Identification. *Recent Advances in Fluid Mechanics, Heat and Mass Transfer and Biology* (WSEAS Press, 163 p), pp 23-29, 2011.
6. Volkov K.N. Visualization methods of vertical flows in computational fluid dynamics and their applications. *Scientific and Technical Journal of Information Technologies, Mechanics and Optics*, **91** 3, 2014 (in Russian).
7. Volkov K.N., Emelyanov V.N., Teterina I.V., Yakovchuk M.S. Methods and concepts of vortex flow visualization in the problems of computational fluid dynamics. *Num. Methods and Programming*, **17** 1, 2016 (in Russian).
8. Konstantinovskaya T., Lutsky A. Numerical simulation and visualization of wing vortices. *Scientific Visualization*, Vol. **4**, №2, pp 14-20, 2012.
9. Borisov V.E., Davydov A.A., Konstantinovskaya T.V., Lutsky A.E. Application of scientific visualization tools in the study of supersonic vortex pair. *Scientific Visualization*, Vol. **12**, №4, pp 46-55, 2020. DOI: 10.26583/sv.12.4.05

10. Bykov L.V., Molchanov A.M., Scherbakov M.A., Yanyshv D.S. *Computational mechanics of continuous media in problems of aviation and space technology*. LENAND, 2019, 668 p (in Russian).
11. Hybrid supercomputer system K-60 <https://www.kiam.ru/MVS/resourses/k60.html>
12. Borisov V.E., Davydov A.A., Kydryshov I.Yu., Lutsky A.E. ARES software package for numerical simulation of three-dimensional turbulent flows of viscous compressible gas on high-performance computing systems, Certificate of registration of a computer program RU 2019667338, (23 December 2019) (in Russian).
13. Allmaras S.R., Johnson F.T., Spalart P.R. Modifications and Clarifications for the Implementation of the Spalart-Allmaras Turbulence Model. *Seventh International Conference on CFD (ICCFD7)*, Big Island, Hawaii (9-13 July 2012).
14. Edwards J.R., Chandra S. Comparison of eddy viscosity-transport turbulence models for three-dimensional, shock-separated flow fields. *AIAA Journal* **34** 4, pp 756–763, 1996.
15. Borisov V.E., Lutsky A.E. Simulation of transition between regular and Mach shock waves reflections by an implicit scheme based on the LU-SGS and BiCGStab methods. *KIAM Preprint* **68** (2016) DOI: 10.20948/prepr-2016-68 (in Russian).
16. Haller G. An objective definition of a vortex. *J. Fluid Mech.*, **525**, pp 1-26, 2005.
17. Kolář V. Vortex identification: New requirements and limitations. *International Journal of Heat and Fluid Flow*, **28**, pp 638–652, 2007.
18. Jeong J., Hussain F. On the identification of a vortex. *Journal of Fluid Mechanics*, **285**, pp 69–94, 1995.
19. Strawn R.C., Kenwright D.N., Ahmad J. Computer visualization of vortex wake systems. *AIAA Journal*, **37** 4, pp 511–512, 1999.
20. Forster K.J., Barber T.J., Diasinos S., Doig G. Interaction of a counter-rotating vortex pair at multiple offsets. *Experimental Thermal and Fluid Science J.*, **86**, pp 63-74, 2017.
21. Saffman P.G. *Vortex Dynamics*. Cambridge: Cambridge Univ. Press, 1993, 311 p.
22. Wang Y., Liu P., Hu T., Qu Q. Investigation of co-rotating vortex merger in ground proximity. *Aerospace Sciences and Technology*, **53**, pp 116-127, 2016.
23. Hunt J.C.R., Wray A.A., Moin P. Eddies, stream, and convergence zones in turbulent flows. Technical Report № CTR-S88. Palo Alto: Center for Turbulent Research, pp 193–208, 1988.
24. Liu C., Gao Y., Tian S., Dong X. Rortex—A new vortex vector definition and vorticity tensor and vector decompositions. *Phys. Fluids*, 2018, **30**, 035103.
25. Shrestha P., Nottage C., Yu Y., Alvarez O., Liu C. Stretching and shearing contamination analysis for Liutex and other vortex identification methods. *Advances in Aerodynamics*, **3** 8, 2021.